Offspring size resolves a latitudinal population growth rate paradox in rays and skates

Ellen Barrowclift[1*], Jennifer S. Bigman[2], Eric D. Digel[3], Per Berggren[1*], Nicholas K. Dulvy[3]

[1]School of Natural and Environmental Sciences, Newcastle University, Newcastle-upon-Tyne, United Kingdom.

[2]Alaska Fisheries Science Center, NOAA, Seattle, United States.

[3]Earth to Ocean Research Group, Department of Biological Sciences, Simon Fraser University, Burnaby, British Columbia, V5A 1S6, Canada.

[*]Corresponding authors: e.barrowclift-mahon@newcastle.ac.uk and per.berggren@newcastle.ac.uk

Key words: Chondrichthyes, metabolic theory, life history theory, population growth rate, temperature size rule

Abstract

As animal populations continue to decline, understanding global patterns of life histories will improve our predictions of species vulnerability and extinction risk to prioritise management. Sharks and rays are threatened with extinction due to overfishing, particularly in the tropics and sub-tropics. Metabolic theory suggests that warm-water species and populations will have a higher maximum intrinsic rate of population increase (r_{max}) and therefore will be less intrinsically sensitive to exploitation. However, recent empirical work has highlighted a paradox and shown that warm, shallow-water tropical rays have lower r_{max} than cold, deep-water temperate skates. We test whether the different reproductive strategies of live-bearing rays and egg-laying skates explain this observed paradox by comparing variation in r_{max} with adult body mass, offspring size, temperature, and depth across 85 species of rays and skates. Our results show that the large relative offspring size of warm, shallow-water tropical rays better explains their greater intrinsic sensitivity (lower r_{max}) compared to cold, deep-water temperate skates. This is consistent with life history theory that suggests r_{max} is greater in species with smaller relative offspring size. We hypothesise that the larger relative offspring size may be driven by greater predation risk in the tropics and may help explain global patterns of intrinsic sensitivity to overexploitation.

1. Introduction

A key challenge is understanding the diversity of life across the earth. Much focus has been on global patterns of species richness, however, in an era of global change, we also need to understand such patterns of life histories to predict the risk of extinction due to climate change and overfishing. Latitudinal patterns in life histories are largely mediated by temperature, e.g. Bergmann's rule, which states that endotherms in cooler environments will be larger [1]. Similarly, the Temperature-Size Rule (TSR) describes the observed pattern that ectothermic species and populations will generally grow faster to a smaller size-at-maturity (and presumably, smaller adult size) in warmer temperatures [2–4]. Physiologically, as waters warm, metabolic rate and, therefore oxygen demand, increase faster than oxygen availability [5–7]. Metabolic rate is intrinsically linked to an organism's life history and population dynamics due to energy allocation and trade-offs between survival, growth, and reproduction [8–10]. Organisms in warmer waters with higher metabolic rates will tend to have 'faster' life histories than those with slower metabolic rates in cooler waters [8,11,12]. These temperature-related patterns of biogeography are supported by the larger maximum body sizes, larger size-at-maturity, slower growth rates, and longer generation times of organisms at higher, cooler latitudes compared to lower, tropical latitudes [13–15]. It would therefore be expected that population growth rates would be lower at higher, cooler latitudes than at warmer, tropical latitudes, with the inference that higher latitude species and populations are more sensitive to exploitation.

Metabolic scaling expectations suggest that the maximum intrinsic rate of population increase (r_{max}) will scale with body mass with an exponent of -0.25 and that after controlling for body size, r_{max} should increase with temperature [16,17]. This has been shown empirically among populations and across species [18,19]. In line with metabolic theory, a positive relationship between r_{max} and temperature exists across many eukaryote taxa, including fishes such as Atlantic cod (*Gadus morhua*) [16,20]. Further, the biogeography of tuna and mackerel (Scombridae) life histories was found to explain their population trajectories. Cooler, high-latitude species that had slower life histories had experienced greater declines than warmer, lower-latitude species with faster life histories [21,22]. More generally, the ratio of production to biomass (P:B) changes systematically with latitude across the world's fish communities. In the tropics, there is high production and low standing biomass compared to lower production and higher standing biomass in cooler temperate and polar latitudes [23]. Thus, understanding the metabolic basis for life histories such as somatic growth [8] and population growth rate [12] holds promise for understanding global change [12,20,24].

The negative quarter power (-0.25) body mass-scaling of r_{max} assumes that offspring size is proportional to adult size in mammals and elasmobranchs but not for broadcast spawning molluscs and teleost fishes ('the relative offspring size hypothesis') [25,26]. The key question is whether the relative offspring size hypothesis has utility in explaining the diversity of r_{max} across species. The superorder Batoidea (rays and skates) offer the unique opportunity that reproductive mode, and therefore offspring size and number, varies within a diverse evolutionary radiation. Paradoxically, warm, shallow-water tropical rays have lower r_{max} (and hence, are more intrinsically sensitive to overfishing) than cold, deep-water temperate skates with higher r_{max} [27]. Most tropical rays are live-bearers with very low fecundity and larger offspring compared to cooler-water skates that lay numerous eggs with smaller offspring size [28,29]. This could mean that for two species with the same adult body mass, one with larger offspring (and fewer of them) may have a lower r_{max} and therefore *relative* offspring size could affect the scaling of r_{max} [25]. As such, we propose that batoids are an ideal taxon to test how offspring size influences the negative quarter-power body mass-scaling of r_{max} and further, that offspring size may resolve the latitudinal paradox of r_{max} in rays and skates.

Previous studies examining r_{max} across species have generally included adult body mass in their models. However, the relative offspring size hypothesis suggests that it may be offspring

body mass relative to adult body mass that influences the scaling of r_{max}, at least for some taxa. Here, we ask whether larger offspring size explains lower r_{max} in warm, shallow-water tropical rays compared to cold, deep-water temperate skates. We specifically explore whether (1) offspring body mass; (2) offspring body mass and adult body mass; and (3) offspring body mass relative to adult body mass better explains variation in r_{max} compared to adult body mass, temperature, and depth for 85 batoid species.

2. Material and Methods

First we describe the calculation of r_{max}, including the source of the life history data used in the calculations. Second, we describe the source of adult and offspring body mass data, as well as environmental temperature and depth data. Third, we summarise our analytical approach, including the statistical models used to assess different hypotheses of how r_{max} may vary with adult and offspring body mass, temperature, and depth.

(a) Source of life history data and calculation of r_{max}

Female age at 50% maturity (years; α_{mat}), maximum age (recorded for females where known, years; α_{max}), and annual reproductive output (number of female offspring assuming 1:1 sex ratio; *b*) for 85 ray (Torpedo rays, Torpediniformes; Rhino rays, Rhinopristiformes; and stingrays, Myliobatiformes) (n=53) and skate (Rajiformes) (n=32) species were sourced from a published life history database compiled in Barrowclift et al. (2023) [30]. r_{max} was calculated using a modified Euler-Lotka model, with a mortality estimator that accounts for survival to maturity [31,32] (see 'Supplementary methods for calculating r_{max}' in Supplementary Materials'). The modified Euler-Lotka model aims to improve the estimation of r_{max} by accounting for different juvenile survival rates due to different reproductive strategies in sharks and rays [31,32]. However, it is important to note that juvenile survival is likely to be lower in egg-laying skates that are more fecund and higher in live-bearing rays that produce fewer offspring [33,34].

(b) Source of body mass, environmental temperature, and depth data

Estimates of adult body mass (maximum weight in grams) for the 85 species were also sourced from the published life history database compiled in Barrowclift et al. (2023) [30]. Offspring body mass (in grams) was estimated from offspring length (total length or disc width in cm) (note, this is hatching size for skates) reported in Rays of the World [35], Sharkipedia [36], and IUCN Red List Assessments [37]. Where offspring length data were unavailable for a species (n=14), offspring length was estimated from a similar species with similar maximum length and body shape [30]. The median offspring length was used where minimum and maximum offspring lengths were reported. The corresponding offspring body mass was then calculated using length-weight regressions extracted from FishBase using the package *rfishbase* [30,38,39]. Length-weight regressions were selected for females where possible. If length-weight regression coefficients were unavailable, estimates for a closely related species with similar body shape and maximum size were used.

Median depth and environmental temperature for the 85 ray and skate species were also used from Barrowclift et al. (2023). Median depth estimates for each species were taken from depth ranges of IUCN Red List assessments as compiled in Dulvy et al. (2021). Temperature-at-depth data were determined by overlaying a given species' distribution, using species range data shape files that were sourced from https://www.iucnredlist.org/ as compiled in Dulvy et al. (2021), with the International Pacific Research Center's interpolated dataset of gridded mean annual ocean temperatures, which is based on measurements from the Argo Project (data available at http://apdrc.soest.hawaii.edu/projects/Argo/data/statistics/On_standard_levels/Ensemble_mean/1x1/m00/index.html). Temperature grid points were extracted across the species'

distribution from the depth level that was closest to the species' median depth and finally, the median temperature was calculated.

(c) Statistical analyses

Metabolic scaling expectations for how r_{max} relates to body mass and temperature [16] can be estimated with the following linear model:

$$\ln(r_{max}) = \beta_0 + \beta_1 * \ln(M) + \beta_2 * 1/k_B T \,, \quad (1)$$

where r_{max} is the maximum intrinsic rate of population increase (year^{-1}), β_0 is the intercept, β_1 is the body mass-scaling coefficient, M is adult body mass in grams, β_2 is the activation energy E, T is the temperature (in Kelvin), and k_B is the Boltzmann constant (8.617×10^{-5} eV).

In order to consider offspring body mass relative to adult body mass, we include a term for adult-to-offspring size ratio ($M/M_{offspring}$) following Denéchère et al. (2022) in some models. Hence, for the same adult body mass, larger offspring size would lead to a smaller adult-offspring size ratio. Using an information-theoretic approach, we include six additional models representing alternative hypotheses of how r_{max} may vary with (1) offspring body mass $M_{offspring}$ (2) $M_{offspring}$ and adult body mass, and (3) adult-to-offspring size ratio ($M/M_{offspring}$), and compare these with 24 models representing hypotheses of how r_{max} may vary with adult body mass, temperature, and depth from Barrowclift et al. (2023) [40] (Table S1 in the Supplementary Materials). The top models were the same and therefore we only present the 16 most relevant models in our results (Table 1). r_{max}, adult body mass, and offspring body mass data were natural log-transformed and temperature and depth data were standardised (scaled and centred) prior to analyses. A random phylogenetic tree from the distribution of trees in Stein et al. (2018) (available at Vertlife.org) was included as a random effect of phylogeny in all models, with binomial nomenclature updated to reflect current taxonomic nomenclature. Models were fitted with an additional ten random trees to test the sensitivity of results to slight variations in the phylogenies; the results were nearly identical with the same top model, and therefore, results were reported for a single tree (Table S2 in the Supplementary Materials). The phylogenetic position of two species was not known (*Aetobatus narutobiei* and *Maculabatis ambigua*), and therefore, two closely related species (*A. flagellum* and *M. gerrardi*, respectively) were used instead.

Phylogenetic generalised linear models were fitted using the *pgls* function in the *caper* package [42], accounting for non-independence of closely related species. Models were also fitted without data (n=2) for two manta ray species (*Mobula alfredi* and *M. birostris*) with the largest offspring body masses to test sensitivity of results to their removal. The top models were the same and therefore results were presented for the full 85 species dataset (Table S3 in the Supplementary Materials). Adult and offspring body mass were positively correlated (Pearson's r = 0.75) above a threshold of 0.7 in which collinearity severely distorts model estimation [43]. Inverse temperature and depth were also positively correlated (Pearson's r = 0.75). Variance-inflation factors (VIF) were estimated to assess collinearity for all coefficients in the models using the *car* package [44]. VIF values were less than 2, except as expected when interactions were included, indicating that our models were robust to collinearity. The corrected Akaike Information Criterion (AICc) were used to compare models. If including a parameter improved the model's AICc by less than two units (ΔAICc ≤ 2), it was considered relatively uninformative [40,45]. All analyses were run in R version 4.1.2 [46] in RStudio [47].

Table 1: The 16 models examined with associated hypotheses for how maximum intrinsic rate of population increase (r_{max}) varies with adult body mass M, offspring body mass $M_{offspring}$, inverse temperature $1/k_BT$, and depth. Comparison of models using corrected Akaike Information Criteria (AICc), number of parameters (n), negative log-likelihood (-LL), adjusted R^2, difference in AICc from the top model (ΔAICc), and Akaike weights. Models are ordered by ascending AICc, with models with AICc < 2 shown in bold.

Hypothesis	Model: $\ln(r_{max})$ ~	n	-LL	AICc	R^2	Adj. R^2	ΔAICc	Weights
r_{max} varies with adult and offspring body mass and temperature	**$\ln(M) + \ln(M_{offspring}) + 1/k_BT$**	**4**	**-63**	**134.4**	**0.21**	**0.18**	**0**	**0.356**
r_{max} varies with offspring body mass only	**$\ln(M_{offspring})$**	**2**	**-65.4**	**135**	**0.17**	**0.16**	**0.6**	**0.264**
r_{max} varies with adult and offspring body mass	$\ln(M) + \ln(M_{offspring})$	3	-65.3	136.9	0.17	0.15	2.5	0.102
r_{max} varies with adult and offspring body mass, and the effect of mass scaling coefficient varies with offspring size	$\ln(M) * \ln(M_{offspring})$	4	-64.9	138.2	0.17	0.14	3.8	0.053
r_{max} varies with adult body mass and temperature	$\ln(M) + 1/k_BT$	3	-66.1	138.5	0.14	0.12	4.1	0.046
r_{max} varies with adult body mass and depth	$\ln(M)$ + depth	3	-66.1	138.6	0.14	0.12	4.2	0.044
r_{max} varies with adult body mass and the effect of temperature varies with depth	$\ln(M) + 1/k_BT$ * depth	5	-64.1	138.9	0.18	0.14	4.5	0.038
r_{max} varies with adult body mass, temperature, and depth	$\ln(M) + 1/k_BT$ + depth	4	-65.4	139.3	0.16	0.13	4.9	0.031
r_{max} varies with adult body mass and temperature, and the effect of mass scaling coefficient varies with temperature	$\ln(M) * 1/k_BT$	4	-65.7	139.8	0.16	0.13	5.4	0.024
r_{max} varies with adult body mass only	$\ln(M)$	2	-68	140.2	0.1	0.09	5.8	0.02
r_{max} varies with adult body mass and depth, and the effect of mass scaling coefficient varies with depth	$\ln(M)$ * depth	4	-66.1	140.8	0.14	0.11	6.4	0.015
r_{max} varies with (inverse) temperature only	$1/k_BT$	2	-69.5	143.1	0.07	0.06	8.7	0.005
r_{max} varies with depth only	depth	2	-70.3	144.8	0.05	0.04	10.4	0.002
r_{max} varies with adult to offspring size ratio and temperature	$\ln(M/M_{offspring}) + 1/k_BT$	3	-69.2	144.8	0.08	0.06	10.4	0.002
average r_{max} (i.e. intercept-only model)	1	1	-72.7	147.5	0	0	13.1	0.001
r_{max} varies with adult to offspring size ratio only	$\ln(M/M_{offspring})$	2	-72.7	149.5	0	-0.01	15.1	0

3. Results

Of 16 models examined, the top model was for r_{max} varying with adult body mass, offspring body mass, and temperature (ΔAICc = 0), describing the greatest amount of variation in r_{max} across species (adjusted R^2 = 0.18) [40] (Table 1). The second-ranked model, which described r_{max} varying solely with offspring body mass, was within 2 AICc units (ΔAICc = 0.6) of the top-ranked model and was more parsimonious. However, this model only had approximately 74% of the support of the top-ranked model (Akaike weights) and accounted for slightly less variation (adjusted R^2 = 0.16). This model had the least uncertainty (smallest confidence intervals) in coefficient estimates for offspring body mass (Figure 1). The effect sizes of offspring body mass and temperature were considered significant as the 95% confidence intervals did not overlap zero (Figure 1). Including adult body mass in the relationship between r_{max} and offspring body mass received moderate support but did not increase ΔAICc by more than two units (ΔAICc = 2.5), with approximately 29% of the support of the top-ranked model and accounting for slightly less variation (adjusted R^2 = 0.15). Including an interaction term between adult and offspring body mass received less support (ΔAICc = 3.8), with approximately 15% of the support (Akaike weights) of the top-ranked model and no increase in variation explained (adjusted R^2 = 0.14). The remaining models were not well supported (ΔAICc > 4) (Table 1). There was a strong phylogenetic signal from the residuals of r_{max} in all models (Pagel's λ ≥ 0.8) (Table S4 in the Supplementary Materials).

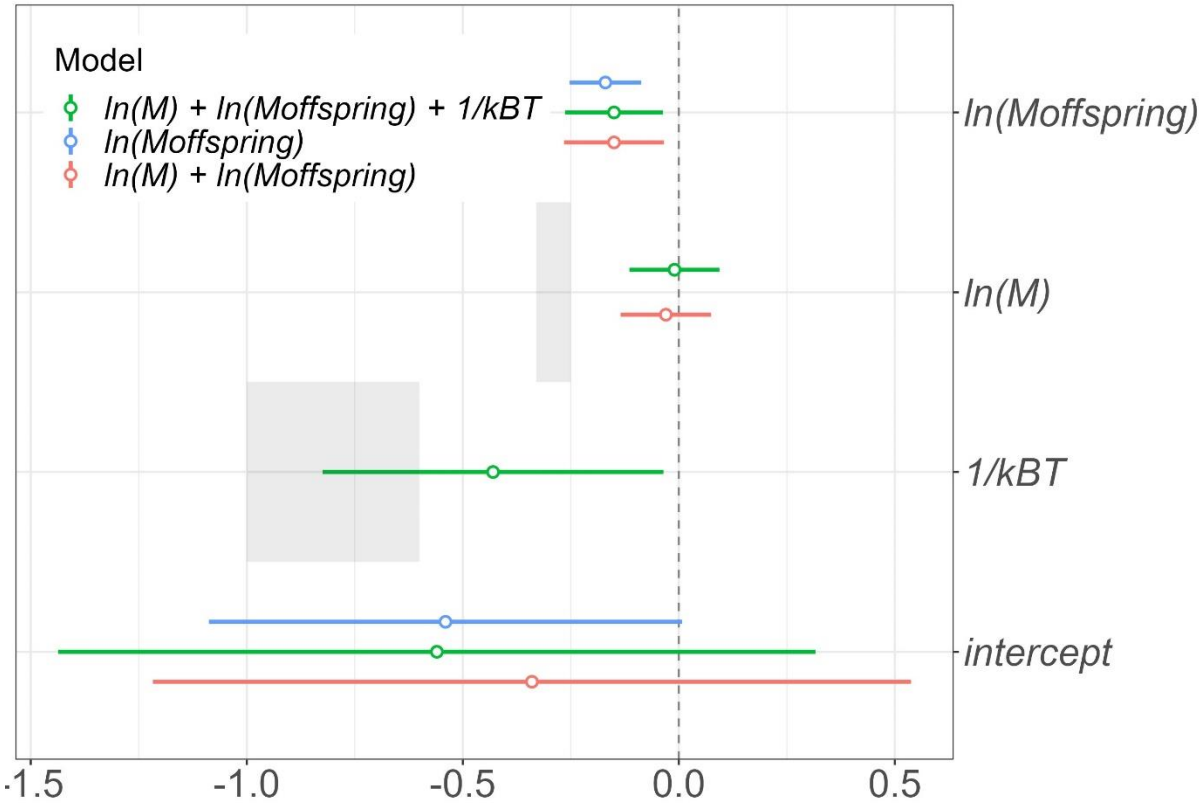

Figure 1: Coefficient plot showing the effect sizes for offspring body mass ($M_{offspring}$), adult body mass (M), and inverse temperature ($1/k_BT$) on r_{max} in the top three models. Error bars show the 95% confidence intervals and effect sizes are considered significant when confidence intervals do not overlap zero. The shaded area shows the expected effect size for adult body mass (-0.33 to -0.25) and temperature (-1.0 to -0.6) based on metabolic theory.

Adult body mass explained more variation in r_{max} when it was the sole mass predictor in the model (Table S4 in the Supplementary Materials). However, once offspring body mass was included as a predictor, variation in r_{max} was mostly explained by offspring body mass, suggesting it is a better predictor of r_{max} compared to adult body mass. There was a negative relationship between r_{max} and offspring body mass for the 85 ray (n=53) and skate (n=32) species (Figure 2a; Table S4 in the Supplementary Materials). There was a positive relationship between adult and offspring body mass (Figure S1a in the Supplementary Materials) and a negative relationship between offspring body mass and median annual fecundity as expected (Figure S1b in the Supplementary Materials). Offspring body mass was generally larger for rays but there was little difference in adult body mass between warm, shallow-water tropical rays and cold, deep-water temperate skates (Figure S2 in the Supplementary Materials). Indeed, the effect of adult body mass on r_{max} was less than expected from metabolic theory (Table S4 in the Supplementary Materials). Larger offspring body mass, relative to adult body mass, resulted in a smaller adult-to-offspring size ratio for rays compared to skates (Figures S2 and S4 in the Supplementary Materials). However, models including the adult-to-offspring size ratio were not well supported compared to those with offspring body mass (Table 1). The effect of inverse temperature $1/k_BT$ and depth were negative across models indicating r_{max} is higher in warmer, shallower water species as would be expected from metabolic theory (Table S4 in the Supplementary Materials). The scaling of temperature with r_{max} overlapped with the expectation from metabolic theory of approximately -0.6 (Figure 1; Table S4 in the Supplementary Materials). However, r_{max} was found to be lower at warmer temperatures (Figure 2a). Yet, despite a weak negative relationship between offspring body mass and temperature for rays and skates (Figure S3a in the Supplementary Materials), shallow, warm-water rays with larger relative offspring tended to have lower r_{max} than deep, cool-water skates with smaller offspring (Figure 2b; Figure S2 in the Supplementary Materials).

4. Discussion

We found evidence that species with larger offspring size relative to adult size, typical of tropical rays, have lower population growth rates. This pattern helps to explain the paradox of why shallow-water tropical rays have lower population growth rates, compared to cold, deep-water temperate skates with smaller offspring. This is in contradiction to the metabolic expectation that faster life histories occur in warmer habitats. Instead, this is more consistent with recent work that suggests the metabolic scaling expectation of r_{max} with body mass is only found when offspring size is considered [25]. Denéchère et al. (2022) found that the scaling of r_{max} varied across taxa and only matched metabolic expectations (-¼) when offspring body mass is proportional to adult body mass (equal adult-to-offspring size ratio). For elasmobranchs specifically, the scaling of r_{max} with adult body mass matched metabolic expectations [25]. However, we found that although the scaling of r_{max} for the group of elasmobranchs we examined -- batoids -- was around -¼, this slope was for offspring body mass and not adult body mass, which did not have a large effect size. Indeed, on average, the effect size of offspring body mass on r_{max} was twice as large as adult body mass. We also posit that the high predation risk in the tropics drives selection of larger adult and offspring body sizes of tropical rays. Next, we consider: (1) how our results differ from the typical temperature and latitudinal patterns in life histories; (2) the evolution of live-bearing and how selection in response to predation risk results in large offspring for tropical rays; and (3) future directions and caveats.

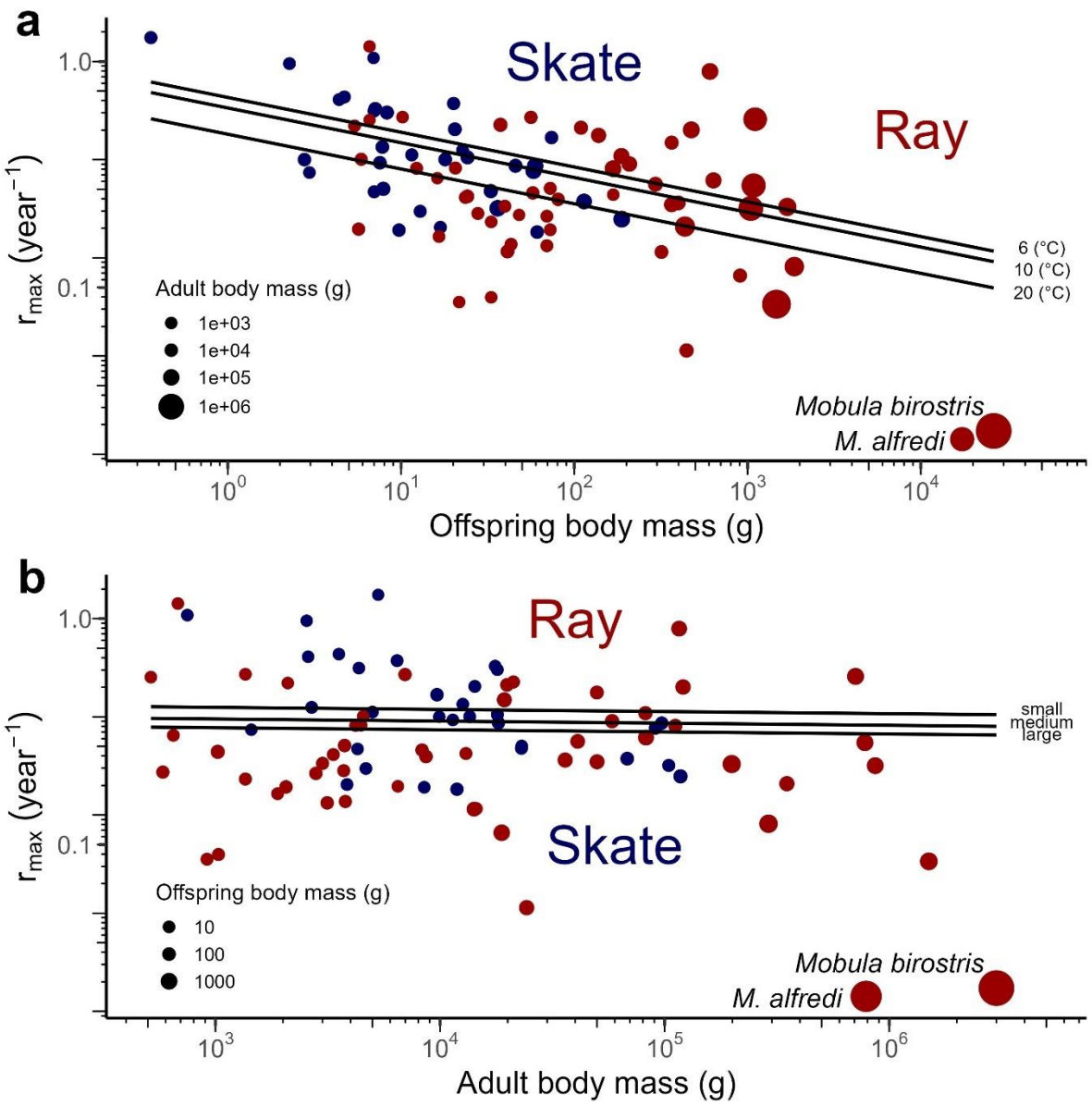

Figure 2: Relationship between maximum intrinsic rate of population increase (r_{max}) and (a) offspring body mass (g) and (b) adult body mass (g) in log10 space for 85 ray (n=53, red points) and skate (n=32, blue points) species. Fitted lines show the predicted relationships for the top model: $\ln(r_{max}) \sim \ln(M) + \ln(M_{offspring}) + 1/k_B T$ across (a) three temperatures (6, 10, 20°C) with fixed median adult body mass and (b) three median offspring weights (small, skates; medium, all species; large; rays) with fixed temperature (10°C). (a) Adult body mass (g) and (b) offspring body mass (g) are shown by the point size. Fitting the top model across different median adult weights (e.g. small, skates; medium, all species; large; rays) does not change the fitted relationship.

Skates are found in cooler waters, either in deep and cool water found on tropical slopes or across depths in temperate and polar waters. Compared to the cold-habitat skates, warm, shallow-water tropical rays have recently been found to have lower r_{max} and therefore greater intrinsic sensitivity to anthropogenic threats such as overfishing [27]. This contrasts with typical metabolic scaling patterns of life histories in relation to temperature and depth. In warmer temperatures, organisms generally grow faster, mature earlier, and attain smaller maximum body sizes resulting in faster generation times and higher production to biomass ratios [13,15,23]. This also leads to latitudinal and depth-related patterns of temperature and size whereby organisms in shallower, warmer, and/or lower latitude waters have higher metabolic rates and therefore 'faster' life histories compared to organisms in deeper, cooler, and/or higher latitude waters [8,11,48]. In sharp contrast however, we found that absolute offspring size disrupted these typical life-history patterns in batoids. Indeed, including offspring size in models had greater support and explained greater variation in r_{max} compared to adult body mass alone, or when including temperature and depth. When offspring size is proportional to adult size, excluding bet-hedging broadcast spawners, offspring size plays a larger role in determining r_{max} than temperature. While this has previously been shown across large taxonomic groups of mammals and sharks [25], the novelty here is that we have shown this effect within a lineage of contrasting offspring sizes. Specifically, the differences in r_{max} between warm, shallow-water rays and cold-habitat skates are likely due to their different reproductive strategies - as live-bearing rays have fewer, larger offspring compared to egg-laying skates with large numbers of smaller offspring - as hypothesised in Barrowclift et al. (2023). This pattern differs from the typical pattern in vertebrates and invertebrates. Generally, offspring size tends to have a negative relationship with temperature due to differences in maternal investment, with females producing larger, better-provisioned offspring in colder environments [49,50]. This large-offspring-in-the-cold pattern is supported by both a cross cohort experiment of bryozoans [49] and a metanalysis spanning 72 species from five ectotherm phyla [50]. Similarly, we found a weak negative relationship between offspring size and temperature for rays and a near flat relationship for skates. However, tropical rays generally have larger offspring sizes than cooler-water, temperate skates. It may be that offspring size is largely independent of temperature for rays and skates, with both employing very different reproductive strategies, raising the question as to why large offspring sizes have evolved in shallow tropical rays.

Live-bearing has been hypothesised to have evolved from egg-laying in order to increase the survival of offspring through a controlled maternal environment and greater protection from predators [28,51]. In live-bearing species, offspring size is constrained by the size of the maternal body cavity but results in offspring with greater survival [52,53]. Whereas in egg-laying species, size is limited by nutrients stored in the yolk sac [54]. The egg-laying reproductive strategy of skates is thought to be advantageous because it requires less energy and shorter reproductive cycles but there will be survival consequences for the offspring due to smaller size, and, thus, greater risk of predation [28]. We found that offspring size had a negative relationship with annual fecundity, reflecting the trade-off between the number and size of offspring [55,56]. We also confirmed the expectation that larger rays tend to have larger and more offspring [55]. Offspring size will affect juvenile survival to maturity, which is important to consider, given the maternal trade-off between lifetime reproductive output, which likely varies between egg-laying and live-bearing reproductive modes [31]. In the calculation of r_{max} for elasmobranchs, there is the pragmatic assumption that juvenile survival to maturity is the same as the survival rate of adult ages (a consistent mortality estimator). However, our key finding suggests the average mortality depends on offspring size, presumably with larger absolute offspring sizes (typical of tropical rays) having lower predation risk than smaller offspring (typical of colder-water skates). This then leads to the question as to why it might be advantageous for tropical warm-water rays to have larger offspring than temperate cold-habitat skates?

The ancestral reproductive mode of sharks and rays is egg-laying with the subsequent evolution of live-bearing and a particularly high degree of maternal investment found in the

shallow-tropical elasmobranch species [29,57]. The diversification and radiation of elasmobranchs throughout shallow tropical shelf seas and the pelagic zone appears to be associated with the evolution of live-bearing and multiple mechanisms for providing additional maternal investment in offspring [29]. The question that remains is why live-bearing with additional maternal investment has evolved. Predation tends to be size-based in the marine realm [58,59]. We speculate that shallow tropical rays have evolved larger offspring in response to selection pressure from greater predation risk in the tropics. We further speculate that this predation risk drove the evolution of live-bearing, and in particular the convergent evolution of multiple forms of matrotrophy. Generally, offspring size is larger in chondrichthyans compared to teleost fishes in which live-bearing appears to have evolved in particularly small-bodied taxa, suggesting the drivers of viviparity are fundamentally different in chondrichthyans [28]. Regarding predation risk, since Darwin, it has long been hypothesised that abiotic effects are more important at higher cooler latitudes whereas biotic interactions are more prevalent in shaping species biology towards the equator [60]. Recent experimental evidence from caged and uncaged epifaunal communities suggests predation rates are greater in shallow, tropical waters than at higher latitudes [61]. Additionally, evidence from Baited Remote Underwater Video (BRUVs) surveys along a gradient of fishing pressure, reveals that the decline of sharks leads to increases in ray abundance, consistent with predation driving community structure on tropical coral reefs [62,63].

Given Bergmann's rule and the Temperature-Size-Rule (TSR), adult body size of temperate skates in cooler waters would be expected to be larger than tropical rays in warmer waters. However, our results suggest there is wide variation in adult body size across rays and skates and, if anything, the tropical rays are, on average, larger than cooler-water skates. We speculate above that the larger offspring sizes and live-bearing are a result of elevated predation in the tropics; given the body cavity constraint on offspring size of live-bearers we further speculate that large offspring size would require the evolution of larger adult body sizes in tropical rays that would allow greater maternal investment. This is consistent with the adult body size differences being the opposite of what might be expected under a TSR hypothesis, i.e. larger in tropical rays and smaller in cool-water skates, and may explain this exception to the TSR where tropical rays attain larger sizes at higher temperatures [64]. Instead, our findings are more consistent with a mortality theory of life histories, and specifically the mortality arising from predation risk and offspring size [10,65].

We found that offspring size explained high variation in r_{max} for rays and skates and is another simple life history trait alongside adult maximum body mass that could be used to estimate r_{max}. Simple variables that are widely available such as these life history traits, environmental temperature, and depth range have the potential to predict population growth rates and therefore extinction risk, fishing limits, and recovery potential, which is especially necessary for data-poor species [27,48]. Empirical estimates of juvenile mortality for sharks and rays are still needed to better understand juvenile survival across species with different reproductive strategies. Whilst the mortality estimator used in the modified Euler-Lotka model to calculate r_{max} accounts for juvenile survival to maturity, size-dependent mortality rates could be explored to investigate differences across reproductive and offspring size strategies. Our results suggest that these differences may be key to understanding biogeographic patterns in extinction risk. We hypothesise that greater predation risk in the tropics has driven the evolution of larger offspring size to increase offspring survival in tropical rays, potentially through live-bearing reproductive mode, increased matrotrophy, and larger adult body sizes. Consequently, shallow-water tropical rays have lower population growth rates and are more intrinsically sensitive to overfishing than may be expected from metabolic ecology.

Data accessibility

The datasets supporting this article are available at FigShare (DOI: https://doi.org/10.6084/m9.figshare.20182109). The code to reproduce the analyses of this

study in R are available at Github (https://github.com/EBarrowclift/batoid-rmax-offspring-scaling).

Funding

EB was funded by a Natural Environment Research Council (NERC) PhD studentship through the IAPETUS2 Doctoral Training Partnership and a UK Research and Innovation (UKRI)-Mitacs UK-Canada Globalink Research Placement. JSB was supported by the National Science Foundation (NSF grant number 2109411). NKD was supported by the Natural Science and Engineering Research Council Discovery and Accelerator Awards (grant numbers 5013566 and 462291) and the Canada Research Chairs program (grant number 1228186).

CRediT author contributions

Ellen Barrowclift: Conceptualisation, Methodology, Formal analysis, Investigation, Validation, Data curation, Writing- Original draft preparation, Writing- Review & Editing, Visualisation, Funding acquisition; Jennifer S. Bigman: Formal analysis, Writing- Reviewing and Editing; Eric D. Digel: Formal analysis, Writing- Reviewing and Editing; Per Berggren: Writing- Reviewing and Editing, Supervision, Funding acquisition; Nicholas K. Dulvy: Conceptualisation, Methodology, Formal analysis, Investigation, Validation, Data curation, Writing- Original draft preparation, Writing- Review & Editing, Visualisation, Funding acquisition, Supervision.

References

1. Bergmann C. 1847 Ueber die Verhältnisse der Wärmeökonomie der Thiere zu ihrer Grösse. *Göttinger Studien* **1**, 595–708.
2. Atkinson D. 1994 Temperature and organism size—A biological law for ectotherms? *Adv Ecol Res* **25**, 1–58. (doi:10.1016/S0065-2504(08)60212-3)
3. Atkinson D, Sibly RM. 1997 Why are organisms usually bigger in colder environments? Making sense of a life history puzzle. *Trends Ecol Evol* **12**, 235–239. (doi:10.1016/S0169-5347(97)01058-6)
4. Atkinson D, Morley SA, Hughes RN. 2006 From cells to colonies: At what levels of body organization does the 'temperature-size rule' apply? *Evol Dev* **8**, 202–214. (doi:10.1111/J.1525-142X.2006.00090.X)
5. Rubalcaba JG, Verberk WCEP, Jan Hendriks A, Saris B, Arthur Woods H. 2020 Oxygen limitation may affect the temperature and size dependence of metabolism in aquatic ectotherms. *Proc Natl Acad Sci U S A* **117**, 31963–31968. (doi:10.1073/PNAS.2003292117)
6. Verberk WCEP, Bilton DT, Calos P, Spicer JI. 2011 Oxygen supply in aquatic ectotherms: Partial pressure and solubility together explain biodiversity and size patterns. *Ecology* **92**, 1565–1572. (doi:10.1890/10-2369.1)
7. Pörtner HO, Bock C, Mark FC. 2017 Oxygen- and capacity-limited thermal tolerance: Bridging ecology and physiology. *J Exp Biol* **220**, 2685–2696. (doi:10.1242/JEB.134585)
8. Wong S, Bigman JS, Dulvy NK. 2021 The metabolic pace of life histories across fishes. *Proceedings of the Royal Society B: Biological Sciences* **288**. (doi:10.1098/rspb.2021.0910)
9. Killen SS, Glazier DS, Rezende EL, Clark TD, Atkinson D, Willener AST, Halsey LG. 2016 Ecological influences and morphological correlates of resting and maximal metabolic rates across teleost fish species. *American Naturalist* **187**, 592–606. (doi:10.1086/685893)

10. Auer SK, Dick CA, Metcalfe NB, Reznick DN. 2018 Metabolic rate evolves rapidly and in parallel with the pace of life history. *Nat Commun* **9**, 6. (doi:10.1038/s41467-017-02514-z)
11. Juan-Jordá MJ, Mosqueira I, Freire J, Dulvy NK. 2013 Life in 3-D: Life history strategies in tunas, mackerels and bonitos. *Rev Fish Biol Fish* **23**, 135–155. (doi:10.1007/S11160-012-9284-4/FIGURES/4)
12. Gravel S, Bigman J, Pardo S, Wong S, Dulvy N. 2024 The metabolic basis of population growth across marine fishes. *Fish and Fisheries* , In Press.
13. Munch SB, Salinas S. 2009 Latitudinal variation in lifespan within species is explained by the metabolic theory of ecology. *PNAS August* **18**, 13860–13864.
14. Blackburn TM, Gaston KJ, Loder N. 1999 Geographic gradients in body size: A clarification of Bergmann's rule. *Divers Distrib* **5**, 165–174. (doi:10.1046/J.1472-4642.1999.00046.X)
15. Beukhof E *et al.* 2019 Marine fish traits follow fast-slow continuum across oceans. *Sci Rep* **9**, 17878. (doi:10.1038/S41598-019-53998-2)
16. Savage VM, Gillooly JF, Brown JH, West GB, Charnov EL. 2004 Effects of body size and temperature on population growth. *Am Nat* **163**, 429–441. (doi:10.1086/381872)
17. Brown JH, Gillooly JF, Allen AP, Savage VM, West GB. 2004 Toward a metabolic theory of ecology. *Ecology* **85**, 1771–1789. (doi:10.1890/03-9000)
18. Bernhardt JR, Sunday JM, O'Connor MI. 2018 Metabolic theory and the temperature-size rule explain the temperature dependence of population carrying capacity. *Am Nat* **192**, 687–697. (doi:10.1086/700114)
19. Luhring TM, Delong JP. 2017 Scaling from metabolism to population growth rate to understand how acclimation temperature alters thermal performance. *Integr Comp Biol* **57**, 103–111. (doi:10.1093/icb/icx041)
20. Myers RA, Mertz G, Fowlow PS. 1997 Maximum population growth rates and recovery times for Atlantic cod, *Gadus morhua*. *Fishery Bulletin* **95**, 762–772.
21. Juan-Jordá MJ, Mosqueira I, Freire J, Dulvy NK. 2015 Population declines of tuna and relatives depend on their speed of life. *Proceedings of the Royal Society B: Biological Sciences* **282**. (doi:10.1098/rspb.2015.0322)
22. Juan-Jordá MJ, Mosqueira I, Cooper AB, Freire J, Dulvy NK. 2011 Global population trajectories of tunas and their relatives. *Proc Natl Acad Sci U S A* **108**, 20650–20655. (doi:10.1073/PNAS.1107743108)
23. Jennings S, Mélin F, Blanchard JL, Forster RM, Dulvy NK, Wilson RW. 2008 Global-scale predictions of community and ecosystem properties from simple ecological theory. *Proceedings of the Royal Society B: Biological Sciences* **275**, 1375–1383. (doi:10.1098/RSPB.2008.0192)
24. Myers RA, Worm B. 2005 Extinction, survival or recovery of large predatory fishes. *Philos Trans R Soc Lond B Biol Sci* **360**, 13–20. (doi:10.1098/RSTB.2004.1573)
25. Denéchère R, van Denderen PD, Andersen KH. 2022 Deriving population scaling rules from individual-level metabolism and life history traits. *Am Nat* **199**, 564–575. (doi:10.1086/718642)
26. Neuheimer AB, Hartvig M, Heuschele J, Hylander S, Kiørboe T, Olsson KH, Sainmont J, Andersen KH. 2015 Adult and offspring size in the ocean over 17 orders of magnitude follows two life history strategies. *Ecology* **96**, 3303–3311. (doi:10.1890/14-2491.1)
27. Barrowclift E, Gravel SM, Pardo SA, Bigman JS, Berggren P, Dulvy NK. 2023 Tropical rays are intrinsically more sensitive to overfishing than the temperate skates. *Biol Conserv* **281**, 110003. (doi:10.1016/j.biocon.2023.110003)
28. Goodwin NB, Dulvy NK, Reynolds JD. 2002 Life-history correlates of the evolution of live bearing in fishes. *Philosophical Transactions of the Royal Society of Biological Sciences* **357**, 259–267. (doi:10.1098/rstb.2001.0958)
29. Mull C, Pennell M, Yopak K, Dulvy N. 2022 Maternal investment evolves with larger body size and higher diversification rate in sharks and rays. *bioRxiv* (doi:2022.2001.2005.475057)

30. Barrowclift E, Dulvy NK. 2023 Life history and maximum weight database for rays (Class Chondrichthyes, Superorder Batoidea) up to June 2022. (doi:10.6084/m9.figshare.20182109.v3)
31. Pardo SA, Kindsvater HK, Reynolds JD, Dulvy NK. 2016 Maximum intrinsic rate of population increase in sharks, rays, and chimaeras: The importance of survival to maturity. *Canadian Journal of Fisheries and Aquatic Sciences* **73**, 1159–1163. (doi:10.1139/cjfas-2016-0069)
32. Cortés E. 2016 Perspectives on the intrinsic rate of population growth. *Methods Ecol Evol* **7**, 1136–1145. (doi:10.1111/2041-210x.12592)
33. Frisk MG, Miller TJ, Fogarty MJ. 2001 Estimation and analysis of biological parameters in elasmobranch fishes: A comparative life history study. *Canadian Journal of Fisheries and Aquatic Sciences* **58**, 969–981. (doi:10.1139/cjfas-58-5-969)
34. García VB, Lucifora LO, Myers RA. 2008 The importance of habitat and life history to extinction risk in sharks, skates, rays and chimaeras. *Proceedings of the Royal Society B: Biological Sciences* **275**, 83–89. (doi:10.1098/rspb.2007.1295)
35. Last PR, White WT, de Carvalho MR, Seret B, Naylor GJP, Stehmann M. 2016 *Rays of the world*. CSIRO Publishing.
36. Mull C *et al.* 2022 Sharkipedia: A curated open-access database of shark and ray life history traits and abundance time-series. *Sci Data* **9**. (doi:10.1038/s41597-022-01655-1)
37. Dulvy NK *et al.* 2021 Overfishing drives over one-third of all sharks and rays toward a global extinction crisis. *Current Biology* **31**, 4773-4787.e8. (doi:10.1016/j.cub.2021.08.062)
38. Boettiger C, Lang DT, Wainwright PC. 2012 rfishbase: Exploring, manipulating and visualizing FishBase data from R. *J Fish Biol* **81**, 2030–2039. (doi:10.1111/J.1095-8649.2012.03464.X)
39. Froese R, Pauly D. 2022 FishBase. World Wide Web electronic publication. www.fishbase.org, (08/2022).
40. Burnham KP, Anderson DR. 2002 *Model Selection and Multimodel Inference: A Practical Information-Theoretic Approach*. 2nd edn. Springer New York. (doi:10.1007/b97636)
41. Stein RW, Mull CG, Kuhn TS, Aschliman NC, Davidson LNK, Joy JB, Smith GJ, Dulvy NK, Mooers AO. 2018 Global priorities for conserving the evolutionary history of sharks, rays and chimaeras. *Nature Ecology & Evolution 2018 2:2* **2**, 288–298. (doi:10.1038/s41559-017-0448-4)
42. Orme D, Freckleton R, Thomas G, Petzoldt T, Fritz S, Isaac N, Pearse W. 2018 caper: Comparative analyses of phylogenetics and evolution in R.
43. Dormann CF *et al.* 2013 Collinearity: A review of methods to deal with it and a simulation study evaluating their performance. *Ecography* **36**, 27–46. (doi:10.1111/j.1600-0587.2012.07348.x)
44. Fox J, Weisberg S. 2019 An {R} Companion to Applied Regression, Third Edition. Thousand Oaks CA: Sage.
45. Arnold TW. 2010 Uninformative parameters and model selection using Akaike's Information Criterion. *J Wildl Manage* **74**, 1175–1178. (doi:10.1111/j.1937-2817.2010.tb01236.x)
46. 2021 *R Core Team*. Vienna, Austria: R Foundation for Statistical Computing. See https://www.r-project.org/.
47. 2021 *RStudio Team*. Boston, MA: RStudio, PBC. See http://www.rstudio.com/.
48. Pardo SA, Dulvy NK. 2022 Body mass, temperature, and depth shape the maximum intrinsic rate of population increase in sharks and rays. *Ecol Evol* **12**, e9441. (doi:10.1002/ece3.9441)
49. Marshall DJ. 2021 Temperature-mediated variation in selection on offspring size: A multi-cohort field study. *Funct Ecol* **35**, 2219–2228. (doi:10.1111/1365-2435.13879)

50. Pettersen AK, White CR, Bryson-Richardson RJ, Marshall DJ. 2020 Linking life-history theory and metabolic theory explains the offspring size-temperature relationship. *Ecol Lett* **22**, 518–526. (doi:10.1111/ele.13213)
51. Wourms JP. 1994 The challenges of piscine viviparity. *Isr J Ecol Evol* **40**, 551–568. (doi:10.1080/00212210.1994.10688772)
52. Musick JA, Ellis JK. 2005 Reproductive Evolution of Chondrichthyans. In *Reproductive Biology and Phylogeny of Chondrichthyes* (ed WC Hamlett), pp. 45–78. Boca Raton: CRC press.
53. Wourms JP, Lombardi J. 1992 Reflections on the evolution of piscine viviparity. *Am Zool* **32**, 276–293. (doi:10.1093/icb/32.2.276)
54. Carrier JC, Pratt HLJr, Castro JI. 2004 Reproductive Biology of Elasmobranchs. In *Biology of Sharks and Their Relatives* (eds J Jeffrey C. Carrier, JA Musick, MR Heithaus), pp. 269–286. Boca Raton, London, New York, Washington, D.C.: CRC Press.
55. Cortés E. 2000 Life history patterns and correlations in sharks. *Reviews in Fisheries Science* **8**, 299–344. (doi:10.1080/10408340308951115)
56. Duarte CM, Alcaraz M. 1989 To produce many small or few large eggs: A size-independent reproductive tactic of fish. *Oecologia 1989 80:3* **80**, 401–404. (doi:10.1007/bf00379043)
57. Dulvy N, Reynolds J. 1997 Evolutionary transitions among egg-laying, live-bearing and maternal inputs in sharks and rays. *Proceedings of the Royal Society of London, B* **264**, 1309–1315.
58. Barnes C, Maxwell D, Reuman DC, Jennings S. 2010 Global patterns in predator-prey size relationships reveal size dependency of trophic transfer efficiency. *Ecology* **91**, 222–232. (doi:10.1890/08-2061.1)
59. Verity PG, Smetacek V. 1996 Organism life cycles, predation, and the structure of marine pelagic ecosystems. *Mar Ecol Prog Ser* **130**, 277–293.
60. Sunday JM, Bates AE, Dulvy NK. 2012 Thermal tolerance and the global redistribution of animals. *Nat Clim Chang* **2**, 686–690. (doi:10.1038/nclimate1539)
61. Ashton G V. *et al.* 2022 Predator control of marine communities increases with temperature across 115 degrees of latitude. *Science (1979)* **376**, 1215–1219. (doi:10.1126/science.abc4916)
62. Sherman C, Heupel M, Moore S, Chin A, Simpfendorfer C. 2020 When sharks are away, rays will play: Effects of top predator removal in coral reef ecosystems. *Mar Ecol Prog Ser* **641**, 145–157. (doi:10.3354/meps13307)
63. Simpfendorfer CA *et al.* 2023 Widespread diversity deficits of coral reef sharks and rays. *Science (1979)* **380**, 1155–1160. (doi:10.1126/science.ade4884)
64. Atkinson D. 1995 Effects of temperature on the size of aquatic ectotherms: Exceptions to the general rule. *J Therm Biol* **20**, 61–74. (doi:10.1016/0306-4565(94)00028-H)
65. Glazier DS. 2023 The relevance of time in biological scaling. *Biology (Basel)* **12**, 1084. (doi:10.3390/biology12081084)